COMPARTMENTALIZATION OF THE SUBMEMBRANE CALCIUM ACTIVITY DURING CALCIUM INFLUX AND ITS SIGNIFICANCE IN TRANSMITTER RELEASE

SANFORD M. SIMON AND RODOLFO R. LLINÁS
Department of Physiology and Biophysics, New York University Medical Center, New York, New York 10016

ABSTRACT Quantitative modeling indicates that, in presynaptic terminals, the intracellular calcium concentration profile during inward calcium current is characterized by discrete peaks of calcium immediately adjacent to the calcium channels. This restriction of intracellular calcium concentration suggests a remarkably well specified intracellular architecture such that calcium, as a second messenger, may regulate particular intracellular domains with a great degree of specificity.

INTRODUCTION

Changes in cytosolic calcium ionic concentration ($[Ca^{++}]_i$) have been proposed as regulating a multitude of basic cellular functions (1). Most of these hypotheses are based on correlations of cellular responses with either changes of extracellular calcium concentration ($[Ca^{++}]_o$), total transmembrane calcium fluxes (I_{Ca}), or cytosolic bulk ($[Ca^{++}]_i$), all of which lack the sufficient detailed spatial and temporal information of local $[Ca^{++}]_i$ to address issues of cell biological or biochemical mechanism. In making these correlations, it is often overlooked that Ca^{++} influxes may be limited to specific regions of the cell surface (as has been shown in muscles [2], neuronal dendrites [3, 4], presynaptic terminals [5–7], paramecia [8–10] and growth cones [4, 11–14]). Furthermore, at a finer level calcium channels are the specialized sites for the voltage-dependent transmembrane calcium influx and thus I_{Ca} does not flow uniformly across the surface membrane even at those sites. Unfortunately, present experimental techniques cannot resolve changes of $[Ca^{++}]_i$ in the submicron or submicrosecond level and thus mathematical modeling is the only approach presently available to address this important problem. The goal of the model presented here is to determine the spatial and temporal limits of the changes in $[Ca^{++}]_i$ near the internal surface of the presynaptic terminal membrane of the squid giant synapse during calcium influx and transmitter release.

We have chosen to focus on the role of calcium in transmitter release not only because of the significance of calcium in synaptic transmission but because depolarization release coupling can serve as a model for examining the physiological significance of localized $[Ca^{++}]_i$ changes in other systems.

In the squid giant synapse the presynaptic I_{Ca} can be measured with a time resolution of tens of microseconds (15–18), while the postsynaptic current can be simultaneously monitored (19), with similar temporal resolution, as an indicator of transmitter release (20, 21). An unambiguous correlation has been demonstrated between the time course and amplitude of the presynaptic I_{Ca} and the postsynaptic response (15, 17, 22, 23). However, the correlation between measurements of presynaptic $[Ca^{++}]_i$ with calcium-sensitive dyes and the postsynaptic response is less clear (17, 24).

Our model examines the microscopic distribution of $[Ca^{++}]_i$ during calcium influx and the relationship between changes of $[Ca^{++}]_i$ and transmitter release. This approach to modeling ionic gradients differs from previous models in two respects: (*a*) It is formulated in the microscopic domain and examines the calcium concentration within hundreds of Angstroms of the membrane. (*b*) It is based on the well-documented view that calcium entry occurs through distinct channels that are independently gated as a probabilistic function of voltage.

Three main predictions arise from the numerical solution of the modeling equations: (*a*) The opening of calcium channels results in spatially restricted large peaks of calcium concentration. (*b*) Steady state concentration of the peaks is achieved very rapidly relative to the open time of the channels. (*c*) A complex relationship exists between the magnitude of the membrane depolarization and the $[Ca^{++}]_i$ change, the greatest local concentration changes occurring for the smallest depolarizations from resting potential.

These computed profiles for $[Ca^{++}]_i$ were incorporated into a general model for transmitter release (22). Release

Dr. Simon's present address is Laboratory of Cell Biology, Box 292, Rockefeller University, 1230 York Avenue, New York, NY 10021.

was considered vesicular (25) and was modeled as a probabilistic function of $[Ca^{++}]_i$. The results obtained with the above assumptions were then contrasted with experimental observations. The results obtained from the model predict that: (*a*) Calcium entry is primarily restricted to within the radius of an average synaptic vesicle. (*b*) The nonlinear properties of transmitter depletion may be explained by the effects of transmembrane voltage on the distribution of calcium influx. (*c*) Modeling transmitter release as a nonlinear function of submembrane $[Ca^{++}]$ can result in predictions that are not consistent with experimental findings. (*d*) Nonlinearities between calcium influx and the rate of transmitter release can be adequately modeled by either (i) the effect of transmembrane voltage on synaptic transmitter depletion or (ii) by assuming that two or more channels adjacent to a vesicle must be simultaneously open to effectuate vesicular release.

The results of the model correlate well with the physiological consequences of calcium entry at the squid synapse and provide a consistent parsimonius description of some of the physiological events triggered by calcium ions. Furthermore, the extreme compartmentalization of the changes of $[Ca^{++}]_i$ during the opening of a calcium channel predicted here, and the aggregation of the channels into strategically located hot spots, suggests that whenever calcium is an essential trigger the precise localization of its entry may be as important as its magnitude. Finally, the nonlinearities between I_{Ca} and $[Ca^{++}]_i$ must ultimately be incorporated in the analysis of the functional role of calcium conductances in all cell types when calcium is suspected of functioning other than as a simple charge carrier. A preliminary note on this research has been published by S. M. Simon, M. Sugimori, and R. R. Llinas (26).

METHODS AND RESULTS

The description of the three-dimensional diffusion of calcium entering through a single open channel has been approached with three different numerical techniques: (*a*) treating the calcium as diffusing through a series of concentric hemispheric shells. (*b*) reducing the spherical diffusion equation

$$\delta C(r,t)/\delta t = D_{Ca} \times (2/r \times \delta C(r,t)/\delta r + \delta^2 C(r,t)/\delta r^2)$$

from three to one spatial dimension by substituting $U(r,t) = r \times C(r,t)$

$$\delta U(r,t)/\delta t = D_{Ca} \times \delta^2 U(r,t)/\delta r^2,$$

where $C(r,t)$ is the calcium concentration as a function of time (t) and distance (r) from the channel pore and D_{Ca} is the diffusion coefficient for calcium (6.0×10^{-6} cm^2/s). (*c*) Modeling the calcium as being injected into one compartment of a three-dimensional Cartesian matrix.

The first two approaches utilized an implicit numerical iteration scheme (27, 28). An explicit iteration was used for the three-dimensional diffusion matrix. To assess the robustness of the results the size of both the temporal and spatial steps were varied from 10^{-11} to 10^{-8} s and 1 to 25 Å, respectively. All approaches assumed that the flux per channel (J) was a decreasing function of membrane depolarization from rest as given by Llinás et al. (16). The maximum elementary current of the channel was taken to be 0.1–0.5 pA in the presence of 10 mM $[Ca^{++}]_o$. The values given by this expression are close in magnitude to recent measurements of single calcium channel fluxes (29). As an additional test the results of the above approaches were compared with an analytical solution for three-dimensional diffusion

$$C(r,t) = \frac{2.0 \times 10^3 \times J}{4.0 \times \pi \times FAR \times D_{Ca} \times r} erfc\left(\frac{r}{2.0\sqrt{D_{Ca} \times t}}\right), \quad (1)$$

where FAR is the faraday and $erfc$ is the complementary error function.

The model incorporated calcium buffer within each compartment with variable buffer concentration, mobility, stoichiometry, and rate constants

$$n \cdot [Ca^{++}]_i + [Buffer] \underset{kb}{\overset{kf}{\rightleftharpoons}} [Buffer \cdot nCa], \quad (2)$$

where Buffer-nCa is the concentration of bound calcium-buffer complex.

To obtain the results presented, we used a buffer with $n = 1$, $k_f = 10^8$ mol/s, $k_d = (k_b/k_f) = 10^{-7}$ to 10^{-6} M, a Buffer concentration of 0–500 mM, although 50 μM was used most frequently (30), and a diffusion coefficient of 10^{-7} cm^2/s (31).

We have used buffering constants measured in the squid axon (30), although it has been suggested that there may be a higher degree of buffering in the presynaptic terminal (32).

Spatial and Temporal Distribution of $[Ca^{++}]_i$ during the Opening of a Single Channel

A three-dimensional isoconcentration surface of the calcium concentration during a channel opening is plotted in Fig. 1 *A*. The steady state $[Ca^{++}]_i$ in the two-dimensional plane immediately under the membrane is plotted as a function of distance from the channel pore for depolarizations of 35 mV (Fig. 1 *C*) and 65 mV (Fig. 1 *D*). A cross section is plotted in Fig. 1 *B* (blue line) and superimposed is the steady state calcium distribution in the presence of a saturable, mobile buffer for calcium (orange bars). The presence of a nonmobile buffer has no effect on the steady state distribution of $[Ca^{++}]_i$.

The transient and steady state $[Ca^{++}]_i$ after the opening of the channel are plotted for 500 Å from the pore (Fig. 2 *A*) and for 50 μm from the pore (Fig. 2 *B*). Over the first few hundred angstroms from the channel pore the concentration is close to steady state within a microsecond of channel opening. Following channel closing, if it is assumed that the calcium concentration decrease is due to diffusion, the peaks of $[Ca^{++}]_i$ near the channel disappear in <1 μs (Fig. 2 *C*). However, the submicromolar shifts dissipate only after seconds (Fig. 2 *D*).

We next evaluated the maximal possible rise of free calcium during continuous calcium entry. Here it was assumed that (*a*) the preterminal has a finite volume unlike the model previously discussed that assumed an infinite volume; (*b*) the membrane lacked transmembrane pumps for the removal of calcium; and (*c*) the I_{Ca} was 200

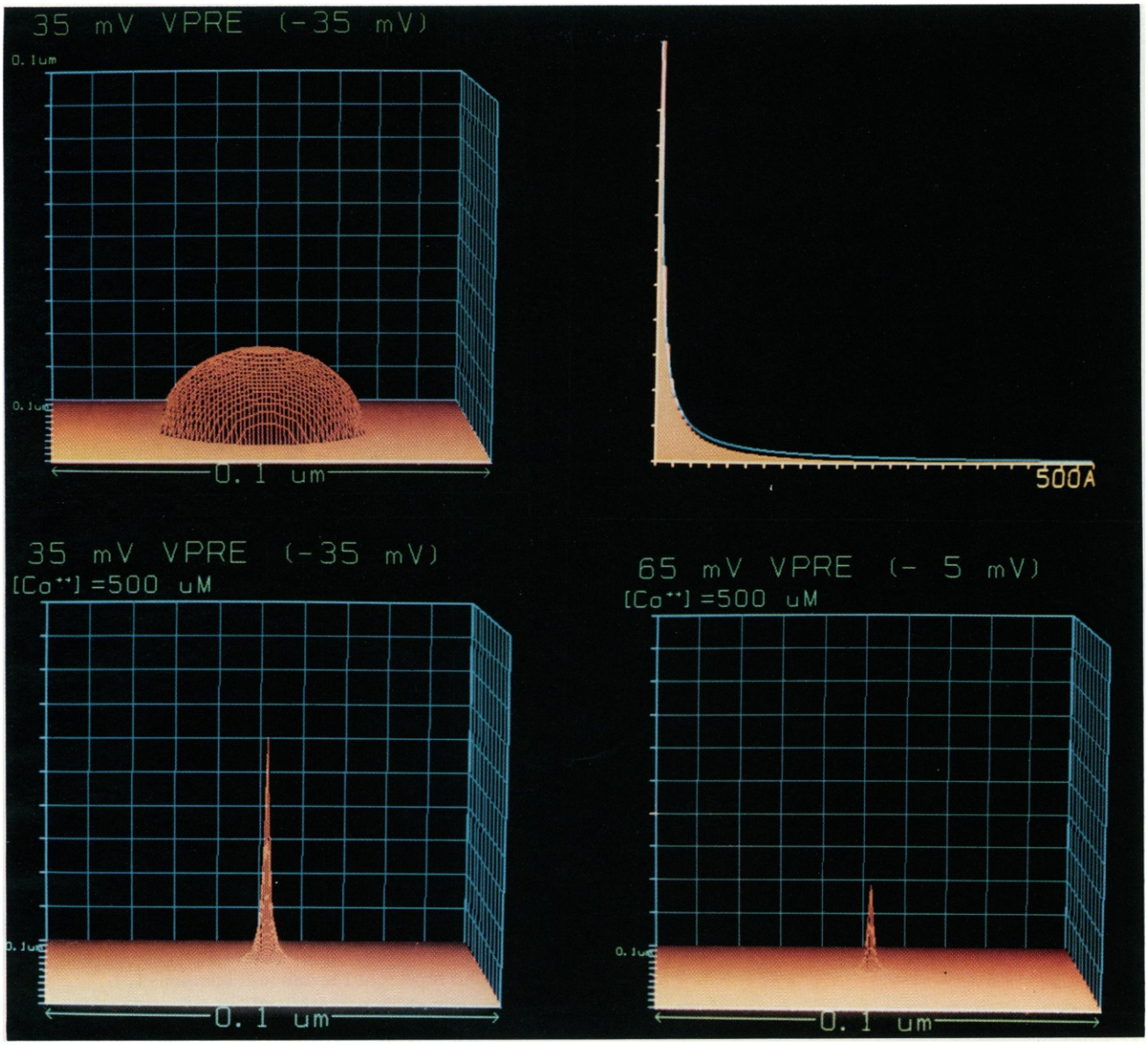

FIGURE 1 Steady state distribution of cytosolic calcium ($[Ca^{++}]_i$) following the opening of a calcium channel. (*A*) A 10 μM isoconcentration surface for $[Ca^{++}]_i$. (*B*) The $[Ca^{++}]_i$ as a function of distance from the pore in the absence of a buffer (solid orange line) and in the presence of a mobile buffer for calcium (bars). The $[Ca^{++}]_i$ in the two-dimensional surface immediately under the membrane is plotted for depolarizations of (*C*) 35 mV and (*D*) 65 mV from a resting potential of −70 mV.

nA per terminal (150 $\mu A/cm^2$, the maximum I_{Ca} measured during a pulse). The magnitude and time course of the average $[Ca^{++}]_i$ is illustrated in Fig. 2 *E* in the presence of 100, 200, and 500 μM buffer for calcium. Under these conditions the time course of $[Ca^{++}]_i$ is substantially slower than the time to peak of calcium concentration at the membrane and the concentrations are accordingly substantially smaller. Thus, the assumption that the terminal may be considered as of infinite volume is only applicable for time periods of milliseconds or shorter. This assumption is made more useful by further assuming the presence of either buffering systems for calcium or transmembrane calcium pumps.

Changes of Cytosolic $[Ca^{++}]$ are Not Linear with Macroscopic I_{Ca}

The results illustrated above demonstrate that $[Ca^{++}]_i$ in the vicinity of the calcium channel is proportional to the calcium flux through a single channel (J) (see Fig. 1 *C,D*) that decreases with depolarization from rest (15, 16). Models, which assume that $[Ca^{++}]_i$ is proportional to the total calcium influx (33–35), predict that $[Ca^{++}]_i$ at the membrane increases with increasing depolarization from rest. However, I_{Ca} is determined by two factors, J and the number of open channels. $[Ca^{++}]_i$ at the membrane is primarily determined by J; thus, increasing the membrane

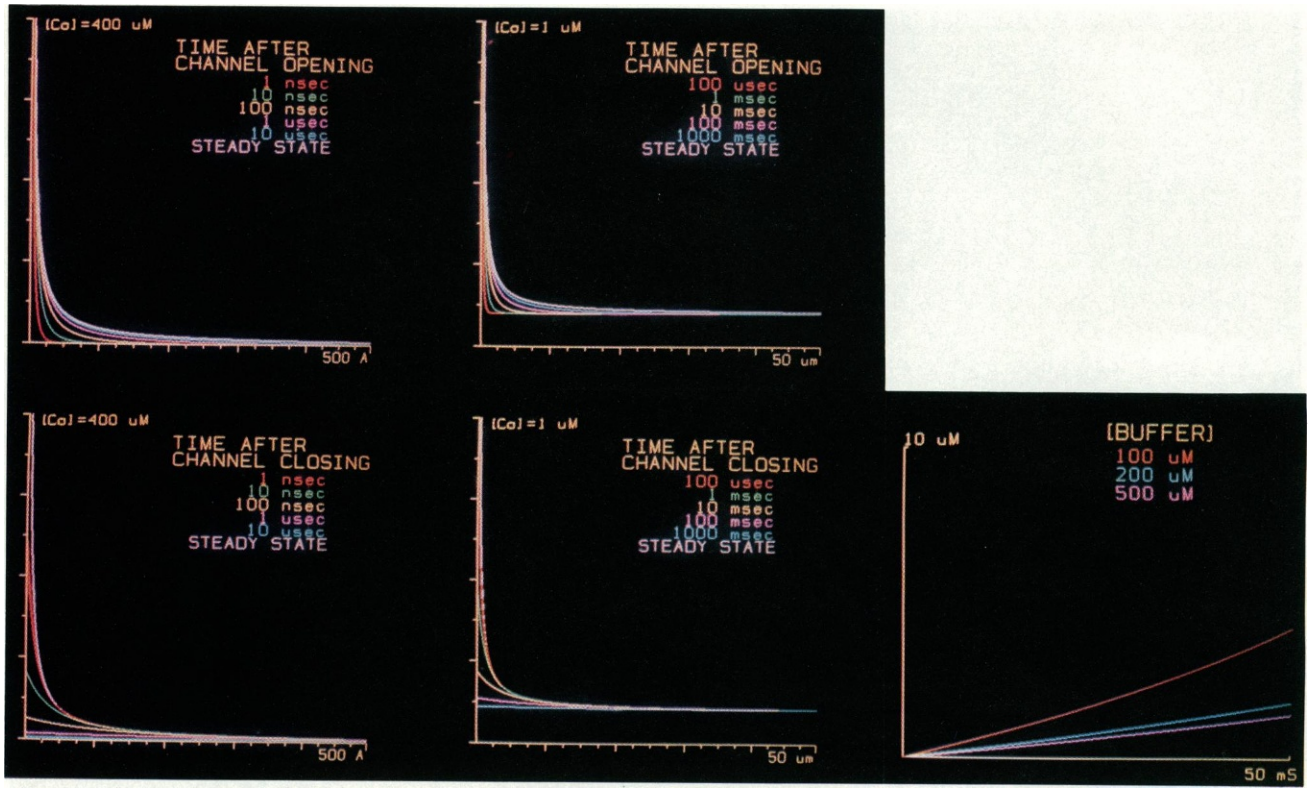

FIGURE 2 Transient and steady state $[Ca^{++}]_i$ after calcium channel opening. In (*A*) plot for the first 500 Å and in (*B*) for the first 50 μm from the channel. Calcium concentration within a few hundred Angstroms of the channel reaches a steady state within microseconds. $[Ca^{++}]_i$ after channel closing was calculated with the assumption that the $[Ca^{++}]_i$ decreased only as result of diffusion. The results are plotted in (*C*) for the first 500 Å and in (*D*) for the first 50 μm from the channel. The large peaks of $[Ca^{++}]$ disappear within microseconds. (*E*) Maximal increase of average $[Ca^{++}]_i$ during long depolarizations assuming a finite volume with no active calcium extrusion. The terminal was assumed to have a buffer for calcium with a K_d of 10^{-6} M and a concentration of 100 μM (orange line), 200 μM (blue line) or 500 μM (pink line).

polarization from -70 to -10 mV increases macroscopic I_{Ca} but decreases the $[Ca^{++}]_i$ under each open channel.

Submembrane $[Ca^{++}]$ under an Active Zone of 900 Channels

The largest calcium flux experimentally determined occurs during the tail current that follows membrane repolarization from a large depolarizing pulse that has opened a large percentage of the calcium channels. In the presence of 10 mM $[Ca^{++}]_o$ the largest I_{Ca} measured is ~5 pA/μm^2. If each channel is assumed to carry a maximum current of 0.5 pA (29) this would correspond to ~10 channels/μm^2 or 1.5 million channels in a typical preterminal. If the calcium channels are assumed to be spread evenly over the presynaptic terminal, then their average separation would be 1,000 Å.

Neither the density nor the distribution of calcium channels is known for the presynaptic terminal of the squid. Nevertheless, freeze-fracture replicas of the presynaptic membrane have revealed the presence of ~1.5 million membrane-bound particles of larger than average size per terminal that form an integral part of the active zone. These particles are aggregated in 1 μm^2 circular patches with a 380 Å separation between particles and have been proposed to represent the calcium channels (6).

To examine the potential effects of concentrating the calcium channels together on submembranous $[Ca^{++}]_i$, our model encompassed 80 active zones each with 900 channels having an interchannel spacing of 300 Å (i.e., slightly more compact than the particles at the active zone). Each channel was modeled as an individual that could randomly open or close. Whether a particular channel shifted from one kinetic state to another depended on both the electric field across the membrane and a number called from a random number table. The modeling tests presented here utilized a six-state (five subunit) kinetic model (15, 16). The intracellular space was modeled as a large three-dimensional rectangular matrix. The bottom surface was adjacent to the plasma membrane with calcium channels localized at regular intervals. If a calcium channel was open during a particular time step, then calcium was added to the box immediately under the channel. This allowed the presence of nonlinear buffers and an examination of the potential interaction of calcium entering from different channels. It also allowed the intro-

duction of anisotropies in the diffusion regime due to membrane effects such as surface charges, or membrane-bound calcium pumps.

The largest flux per open channel and resulting local increase in $[Ca^{++}]_i$ was found for small depolarizations. Under these conditions there was a very low probability for channel opening and the average distance between open channels was relatively large. Larger membrane depolarizations, while increasing the probability of a channel opening, reduced the calcium flux and local $[Ca^{++}]_i$. This minimized the overlap of calcium entering from adjacent channels. Thus, at smaller depolarizations the changes of $[Ca^{++}]_i$ are restricted to a few sites. At larger depolarization the changes of $[Ca^{++}]_i$ are smaller but distributed over more of the inner membrane surface. A model of the distribution of the $[Ca^{++}]_i$ underneath an active zone consisting of 900 channels spaced 300 Å from each other predicted some overlap of steady state calcium in the absence of calcium buffers in the cytosol (Fig. 3 *A*). Increasing the amplitude of the membrane depolarization greatly increased I_{Ca} and filled in the space between the peaks of submembranous $[Ca^{++}]_i$. Indeed while I_{Ca} for a 60 mV depolarization was 17-fold greater than I_{Ca} for a 30 mV depolarization, the peak submembranous $[Ca^{++}]_i$ was smaller, i.e., peak submembranous $[Ca^{++}]_i$ decreased with greater depolarizations. Conditions that decreased the overlap of calcium between channels such as introducing a mobile calcium buffer (Fig. 3 *B*) or increasing the distance between channels further accentuated the inverse relation between depolarization and peak local $[Ca^{++}]_i$.

Comparison with the Results of Previous Models

These results differ from those of previous works in two respects. First, they indicate a much greater degree of localization of the calcium concentration change. Second, they indicate that the presence of a buffer has no effect on the steady state distribution of intracellular calcium near the entry point. The differences between these and previous results can be attributed to a number of assumptions, made by previous authors, that we believe have been inappropriately used. (*a*) Many authors have assumed that the calcium enters diffusely through the membrane (31, 33, 36–38). This eliminates the discrete peaks of high concentration that become obvious when modeling calcium entry through individual channels in the membrane (Fig. 3). (*b*) It has been assumed that the magnitude and time course of the microscopic calcium entry parallels macroscopic conductance change (31, 33, 36–38). This ignores the almost inverse relationship between the voltage dependence of calcium channel activation and calcium entry per open channel. Indeed, as the membrane is depolarized, more channels open but there is also a drastic decrease in the driving force for calcium entry. Since we have taken these parameters into account, the relation between macroscopic calcium currents and the macroscopic calcium concentration changes derived in the present work differ quite substantially from that of previous studies. (*c*) Some authors have quantified the submembrane changes of calcium concentration by assuming that "accumulation of intracellular Ca^{++} can be calculated from the time integral of I_{Ca}, which is directly related to net Ca^{++} entry through Faraday's constant, F. Dividing by the effective intracellular volume (i.e., the volume to which the Ca^{++} is restricted upon entering) yields the increment in concentration (see ref. 39, page 292). When a membrane is depolarized by a 20-ms voltage pulse, their model predicts a resulting submembrane calcium change that is double that elicited by a 10-ms depolarization. This approach ignores two essential points. Once the calcium enters the cell it diffuses away and thus the concentration does not build up indefinitely immediately under the membrane. Second, during the time period of their pulses, channels are continuously opening and closing, but the concentration under any individual channel can only increase during the time period that it is open. (*d*) Most authors have used an analysis of diffusion into a buffered medium that was suggested by Crank (see ref. 40, page 327). If it is assumed that calcium buffering occurs instantaneously (k_f and k_b in Eq. 2 are infinitely large) to an unsaturable buffer with an equilibrium constant k_d, then the diffusion equation

$$\delta C/\delta t = D_{Ca}\nabla^2 C \tag{3}$$

can be rewritten as

$$\delta C/\delta t = D'_{Ca}\nabla^2 C,$$

where D' (the apparent diffusion coefficient)

$$D'_{Ca} = D_{Ca}/(1 + k_b/k_f).$$

However, some of the assumptions underlying this approach are questionable. First, the model predicts large peaks of calcium concentration. Since the buffers for calcium are not of infinite concentration it is possible that the calcium locally saturates the buffer. Second, buffering is a biochemical reaction which, of necessity, must be diffusion limited. Therefore, we question the utility of assuming that the buffering is infinitely fast relative to the time period of the diffusion. Furthermore, the use of numerical iteration requires the use of very small distances within which the calcium concentration is assumed to be equilibrated. Over the 2–5 Å distances used for the compartments in our model the calcium diffusion cannot be considered slow relative to the time course of buffering.

Finally, this approach suggested by Crank has been utilized to yield a number of results that are equivocal. The analytical solution for the diffusion equation in spherical dimensions (Eq. 1) is the product of two terms; the first half represents the steady state distribution of the substance and the second half (the complementary error

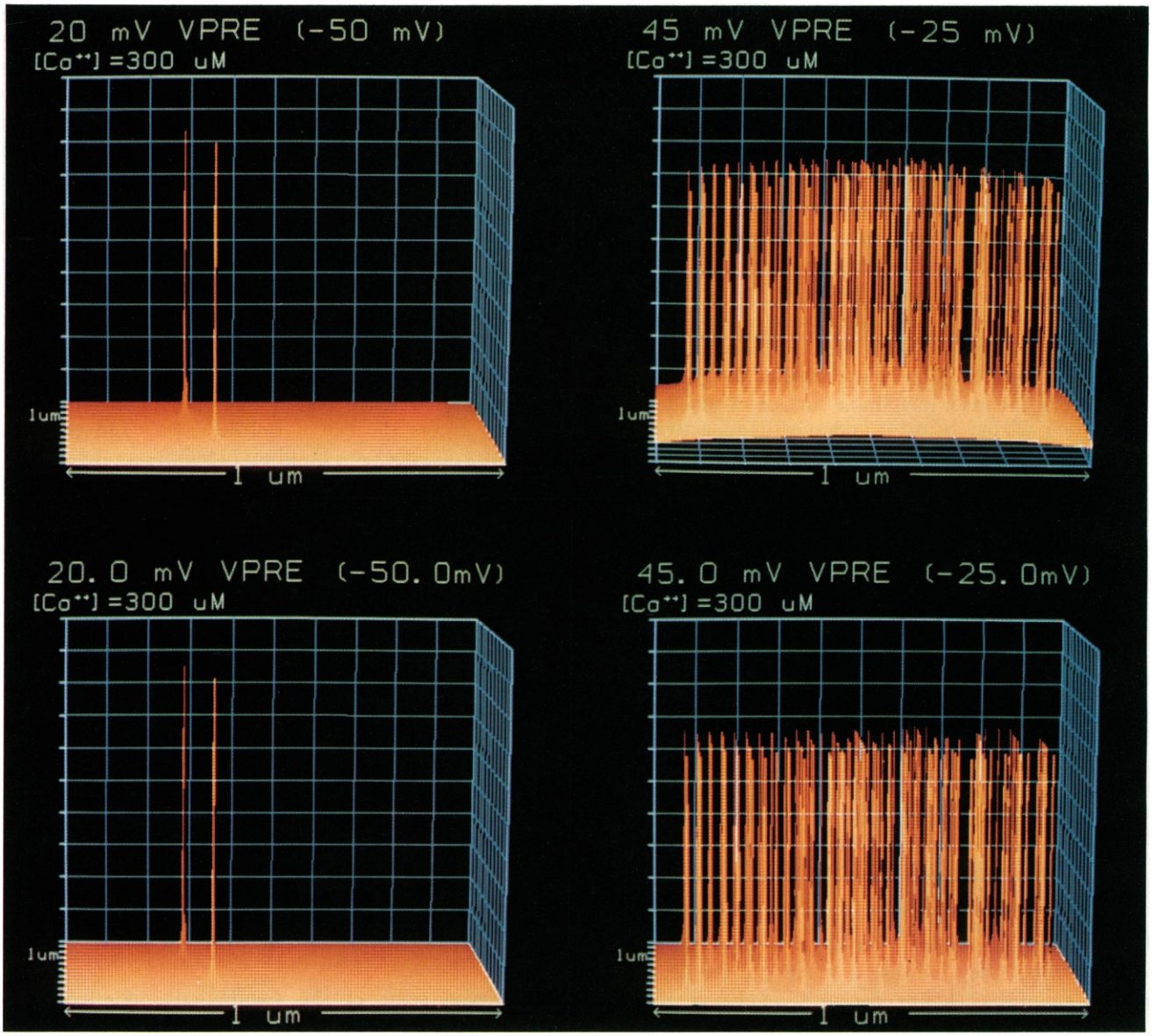

FIGURE 3 Steady state distribution of $[Ca^{++}]_i$ in the two-dimensional surface under an active zone with 900 channels. The channels were assumed to be packed in a rectangular matrix with an interchannel spacing of 300 Å. With increasing depolarization, from a resting potential of −70 mV, the probability of a channel opening increased and the flux per open channel decreased as given by Llinás et al. (15). (*A*) In the absence of a buffer for calcium, the $[Ca^{++}]_i$ is plotted for depolarizations to 20, 45, 70, and 95 mV from the resting potential. (*B*) In the presence of a mobile buffer for calcium, the $[Ca^{++}]_i$ is plotted for depolarizations to 20, 45, 70, and 95 mV.

function term) the time period for the substance to reach its steady state. Some authors (33) have used values for B as large as 40. According to their results, in the steady state, the calcium concentration declines over distance much more gradually (1/41st the rate) in the presence of buffer. Furthermore, by decreasing the apparent diffusion constant (by increasing the buffer concentration) they actually increase the magnitude of the calcium concentration change. Both predictions indicate that there are serious problems with this approach.

If we rewrite Eq. 3 to allow for the presence of a buffer and a source of calcium at the origin, $S_{o,t}$, then the change of calcium due to diffusion is:

$$\delta C/\delta t = D_{Ca} \nabla^2 C + S_{o,t} + k_f C\, Buf - k_b \mathrm{Ca} \cdot buf,$$

where C is the calcium ion concentration, $S_{o,t}$ is a source of calcium at the origin of time t, Buf is the unbound buffer concentration and $Ca \cdot Buf$ is the concentration of bound calcium and buffer.

Using the assumptions presented by Crank, the solution can be expressed in a form in which the diffusion constant D_{Ca} is reduced to D'_{Ca} where

$$D'_{Ca} = D_{Ca}/(1 + k_b/k_f).$$

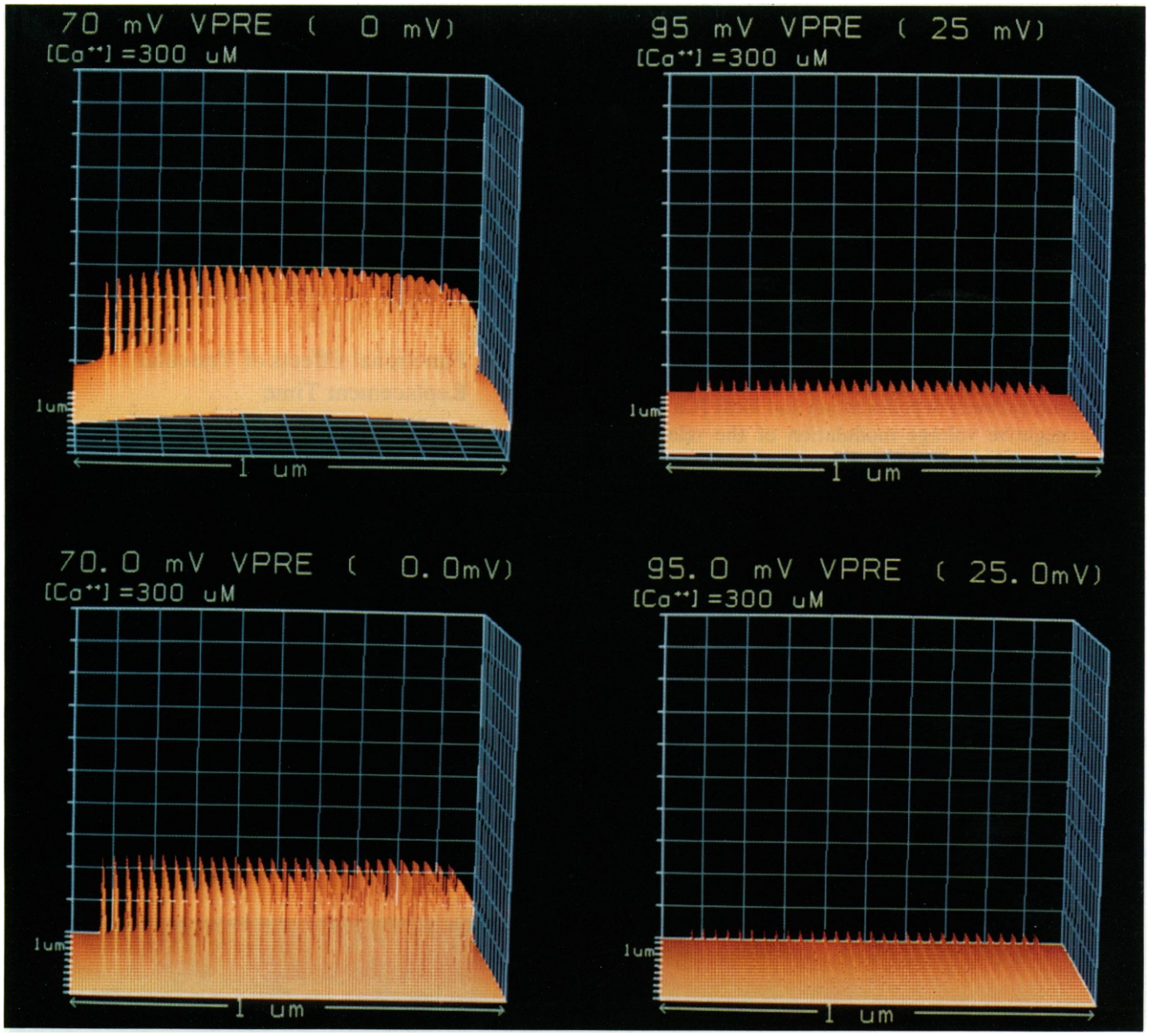

FIGURE 3 Continued.

However, the source term, $S_{o,t}$ must also be reduced to $S'_{o,t}$ where

$$S'_{o,t} = S_{o,t}/(1 + k_b/k_f).$$

Therefore, Eq. 1, the solution to the spherical diffusion equation, can be rewritten as

$$C(r,t) = \frac{2.0 \times 10^3 \times S'_{o,t}}{4.0 \times \pi \times FAR \times D'_{Ca} \times r} erfc\left(\frac{r}{2.0\sqrt{D'_{Ca} \times t}}\right).$$

However, the terms $S'_{o,t}/D'_{Ca} = S_{o,t}/D_{Ca}$ and therefore the solution for the diffusion equation in the presence of a buffer can be written as

$$C(r,t) = \frac{2.0 \times 10^3 \times S_{o,t}}{4.0 \times \pi \times FAR \times D_{Ca} \times r} erfc\left(\frac{r}{2.0\sqrt{D'_{Ca} \times t}}\right).$$

Thus, the presence of a buffer will increase the time period for the substance to reach its steady state (reduce the value of the apparent diffusion constant in the second half of the equation). However, it does not affect the value of the diffusion constant in the first half of the equation and thus does not affect the steady state distribution of $[Ca^{++}]_i$. However, most authors seem to have reduced the apparent diffusion constant in both parts of the equation. Therefore they have predicted a change in the steady state distribution.

Transmitter Release is Best Modeled by a Linear Function of $[Ca^{++}]_i$

The release of transmitter was modeled as a probabilistic function of the submembrane $[Ca^{++}]^n$ where n was

varied from 1.0 to 4.0. Because the locus for calcium's action in transmitter release is unknown, $[Ca^{++}]_i$ was assumed to act (*a*) anywhere immediately under the active zone; (*b*) only directly between the channels; and (*c*) anywhere other than under the channels; or (*d*) the average calcium under a vesicle.

Although depolarizations of 45 and 75 mV from a resting potential (−70 mV) yield the same net I_{Ca}, the resulting predicted distributions of $[Ca^{++}]_i$ are radically different (see Fig. 3). If the stoichiometry of $[Ca^{++}]_i$ in transmitter release is >1, the predicted release is greater at the smaller depolarizations where $[Ca^{++}]_i$ is concentrated in large peaks. The effects of differing stoichiometries for $[Ca^{++}]_i$ on release are shown in Fig. 4. The inverse relationship between depolarization and local $[Ca^{++}]_i$ dictates a negative voltage modulation of the relationship between I_{Ca} and release (Fig. 4 *A*). That is, for increasing levels of depolarization there will be continuously decreasing transmitter release per unit of calcium entry (Fig. 4 *B*). However, all experimental results published to date indicate that an increase of I_{Ca} is always accompanied by an increase in transmitter release (15, 17, 18, 22, 23) and a positive voltage modulation of the release process is the rule (18, 22).

In the model, conditions that accentuate the inverse relation between depolarization and $[Ca^{++}]$ at the release site increase the predicted negative voltage modulation of release. Thus the presence of a mobile calcium buffer reduces the possible overlap of calcium entering from different channels and increases the apparent voltage effects.

Conditions that deemphasize the inverse relation between depolarization and $[Ca^{++}]$ at the release site in the model reduce the negative voltage modulation of release. If it is assumed that the area under the channels (the peaks of the $[Ca^{++}]_i$) does not affect the release process or if the channels are packed closer together, increasing the overlap of Ca^{++}, then the voltage modulation is reduced. The magnitude of the negative voltage modulation decreases as the channels are moved closer until such a point that all of the channels are superimposed.

Functional Effects of Vesicular Replacement Time

The predicted changes of $[Ca^{++}]_i$ are restricted to within a few hundred Angstroms of the channel. Since the vesicles are 300–500 Å in diameter, most channels will only have one vesicle within the range of their calcium flux. Once the vesicle near a given channel is released, then further calcium entry through that particular channel cannot affect release until another vesicle moves into the vacated $[Ca^{++}]_i$ compartment. This predicts a local refractory period for transmitter release produced by the time for replacing a vesicle that has been released, and suggests that the time period for vesicular replacement could be an important variable in synaptic release. Since such replacement time has not, as yet, been determined, the period for replacing vesicles that had been released at individual release sites was varied from 10^{-5}–10^{-1} s, and the results are shown in Fig. 5 for depolarizations of 35 mV (*A*), 65

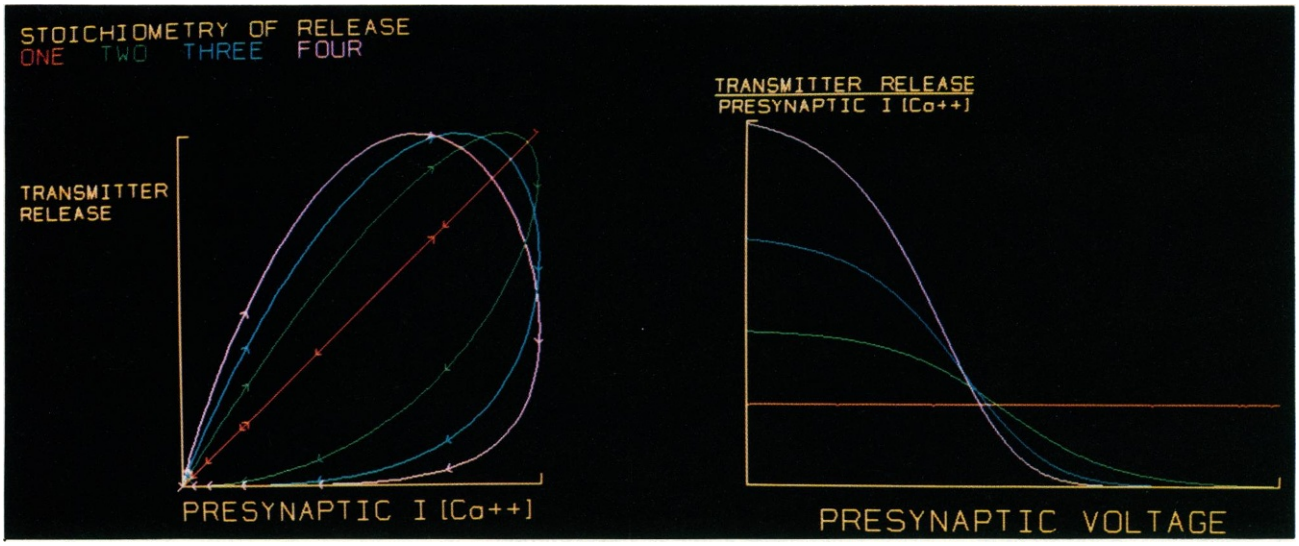

FIGURE 4 The effect of varying the stoichiometry of cytosolic calcium ions to transmitter release on: (*A*) The predicted transmitter release as a function of the presynaptic I_{Ca} assuming that one (orange), two (green), three (blue), or four (pink) calcium ions are needed for each vesicle. Arrows indicate the direction of the plot as the membrane is depolarized. (*B*) Predicted transmitter release per unit of calcium entry as a function of the presynaptic depolarization from resting potential. The amplitude of both the transmitter release and the I_{Ca} have been normalized to their largest values. The presynaptic voltage was varied from zero to 120 mV depolarization from a resting potential of −70 mV.

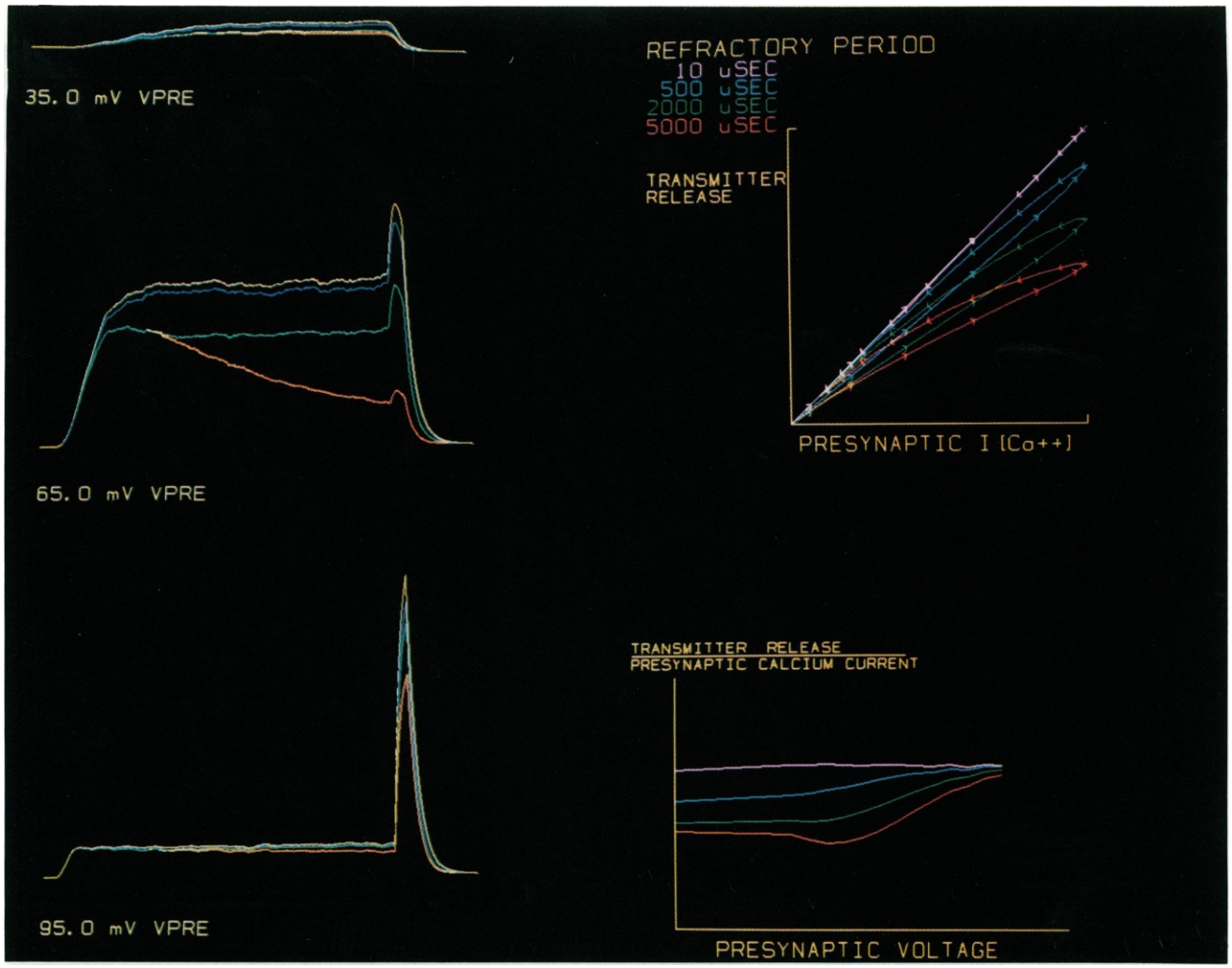

FIGURE 5 The effect of varying the time period for presynaptic vesicular replacement on the predicted postsynaptic response to an 8 ms presynaptic depolarization of (*A*) 35 mV, (*B*) 65 mV, and (*C*) 95 mV from a resting potential of −70 mV. The apparent depletion for a 30 mV depolarization is greater than the depletion at 95 mV, although there has been a greater release of transmitter from the 95 mV depolarization. (*D*) The predicted transmitter release is plotted as a function of the presynaptic I_{Ca}. As the I_{Ca} is increased with increasing depolarization from resting potential there is an apparent positive cooperativity between the I_{Ca} and transmitter release. The amplitude of both the transmitter release and the I_{Ca} have been normalized to their largest values. (*E*) The predicted release per unit of calcium entry is plotted as a function of membrane depolarization from resting potential. Increasing the time delay for replacing a vesicle increases the apparent modulation of transmitter release by the presynaptic voltage. The presynaptic voltage was varied from zero to 120 mV depolarization from a resting potential of −70 mV.

mV (*B*), and 95 mV (*C*). Note that the effects of this replacing time are particularly significant during small depolarizations, where I_{Ca} flows through a few channels.

Indeed, if all calcium entry were to occur through one channel, then after the vesicle near that channel was released, further release could not occur, regardless of increases of $[Ca^{++}]_i$, until the vesicle was replaced. On the other hand, if the same magnitude I_{Ca} were to enter through many channels then calcium could have access to many more vesicles and thus greater transmitter release would ensue. For large depolarizations where many more calcium channels are open there are more vesicles available for release and the effects of the local refractory period are less noticeable. Thus increasing the duration of vesicular replacement results in a voltage modulation of transmitter release. Time periods greater than 100 μs for vesicular replenishment were needed to demonstrate a modulatory effect of voltage on transmitter release that resembled the voltage modulation of transmitter release that has been previously reported in this preparation (Fig. 5 *D*). Periods >3 ms were needed to replicate the time course of synaptic depression (22, 41).

Nearest Neighbors Effect

Because the vesicles are larger (500 Å) than the assumed distance between calcium channels (380 Å), it is possible that a vesicle could be affected by the calcium entry from more than one channel. This assumption does not affect any of the previous results unless it is postulated that for a vesicle to be released it must sense calcium entering

simultaneously from more than one channel. If such a possibility is incorporated into the model, then, as the membrane is depolarized, the probability of a channel opening increases as does the probability that two or more neighboring channels will open under a given vesicle. In such a case the ratio of transmitter release to calcium entry increases with increasing depolarization and there is a positive voltage modulation between I_{Ca} and transmitter release. This is shown in Fig. 6 for release requiring that vesicles must sense two, three, or four simultaneous neighboring channel openings.

DISCUSSION

Modeling of calcium ion movements suggests that the opening of calcium channels results in localized submembrane increases in $[Ca^{++}]_i$. These localized increases are relatively unaffected by the presence of calcium regulatory systems and reach a steady state very rapidly relative to the open time of calcium channels, which is believed to be in the millisecond time domain (29).

When the above findings are introduced into a general model for transmitter release, four predictions emerge: (*a*) There is, of necessity, an intimate relationship between the locus of the calcium channels and the vesicular release apparatus. Thus, as previously indicated, the precise site of calcium influx is a significant parameter in the cell biological role of calcium influx. (*b*) The modeling results are most consistent with experimental findings when a linear relationship between $[Ca^{++}]_i$ and the rate of transmitter release is assumed. (*c*) Vesicular depletion is linearly related to the rate of transmitter release and the experimentally observed nonlinear properties of depletion may be

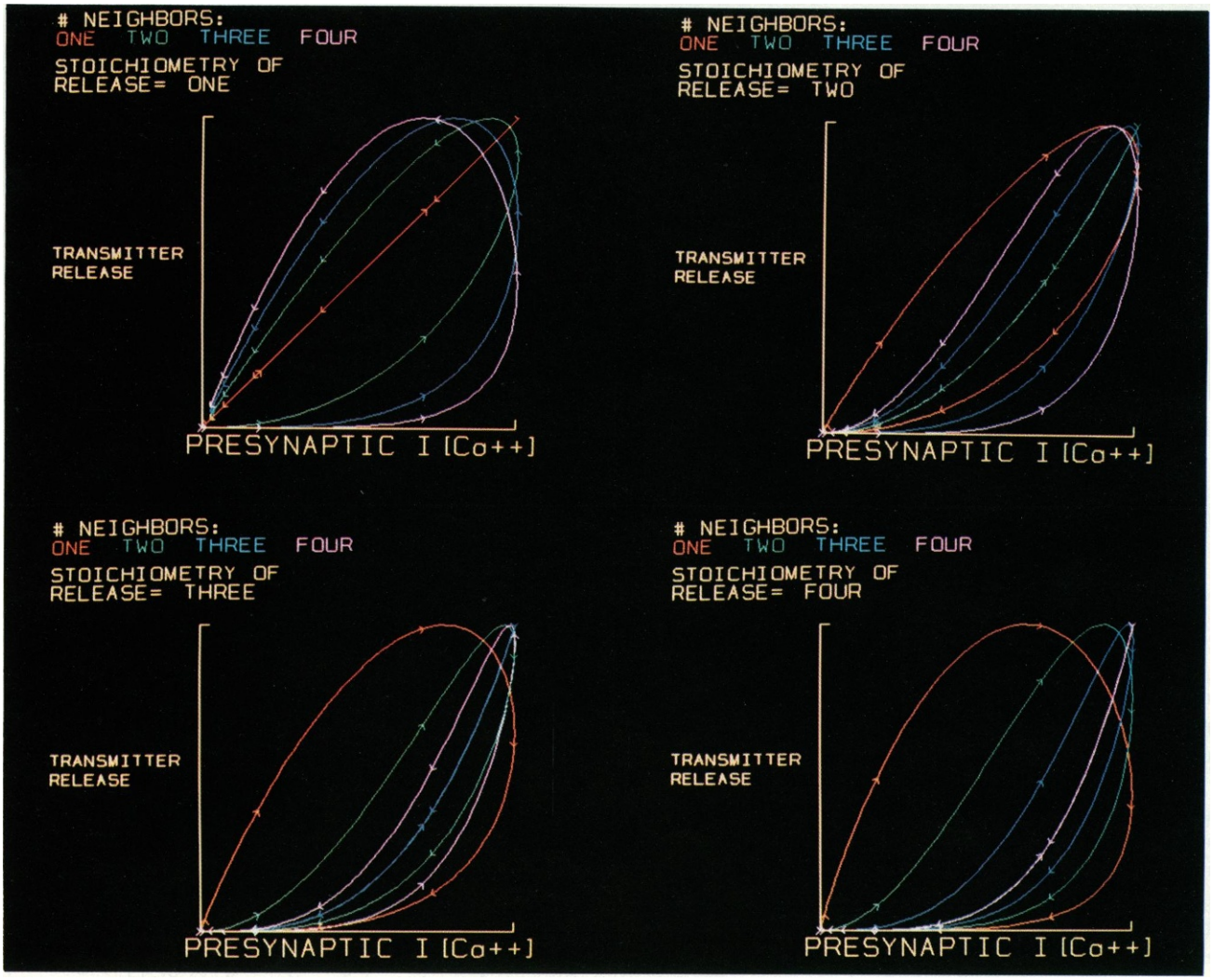

FIGURE 6 The effect on predicted transmitter release assuming that the vesicle must sense the calcium entering from one, two, three, or four channels that are open simultaneously. The release is plotted as a function of the presynaptic I_{Ca} assuming that there is a (*A*) linear, (*B*) second-, (*C*) third-, or (*D*) fourth-order stoichiometry for calcium in transmitter release. The amplitude of both the transmitter release and the I_{Ca} have been normalized to their largest values.

accounted for by the effects of transmembrane voltage on the distribution of calcium entry. (*d*) The nonlinearity between I_{Ca} and transmitter release can be explained as due to either the voltage effects on vesicular replacement time or the necessity that vesicular release be predicated on the simultaneous sensing of calcium entry from more than one channel.

The Site of Calcium Influx

The rather restricted spatial and temporal localization of $[Ca^{++}]_i$ during membrane depolarization implies that transient increases in $[Ca^{++}]_i$ may be effective only immediately adjacent to the site of entry. Since the vesicles are located in significant numbers only in the vicinity of the active zone, it has been previously concluded that their localization is codetermined with that of the calcium channels (32, 6). This is consistent with at least three sets of data from the squid synapse. First, the delay between a step increase in presynaptic I_{Ca} and a postsynaptic response is under 200 μs (15). This gives an upper limit to the total time required for calcium to trigger transmitter release, including vesicular fusion, diffusion of transmitter binding to the postsynaptic receptors, and opening of the postsynaptic channels (42).

Second, the delay between the rapid cessation of I_{Ca} and a decrease in the postsynaptic response is also under 200 μs (Llinás, Sugimori, and Simon, unpublished observations). This indicates that neither free calcium nor calcium bound to an intermediary in release remains elevated in the terminal for much longer than 200 μs. These results and the prediction of the present model are at variance with the "residual free calcium" hypothesis for synaptic facilitation (17, 33, 43–46), which assumes that $[Ca^{++}]_i$ may remain elevated at the release site for hundreds of milliseconds.

Finally, when the presynaptic terminal is invaded by an action potential, the calcium channels open during the repolarization of the terminal, 0.5 ms after the opening of the sodium channels (23). Although some calcium does enter the terminal through the sodium channels (47–49), the sodium conductance can be blocked with tetrodotoxin without affecting either the latency or the magnitude of the postsynaptic response evoked by a simulated presynaptic spike (23). The fact that the calcium entering through the sodium channels does not affect transmitter release supports the view that the changes of $[Ca^{++}]_i$ that trigger transmitter release are highly localized. Taken together, these experimental observations indicate that the site of calcium entry is important for determining its ultimate role in transmitter release (42, 6, 22, 23).

The Model Indicates a Linear Relation between $[Ca^{++}]_i$ and Transmitter Release

Most previous attempts to analyze the stoichiometry of $[Ca^{++}]_i$ to release have adopted a strategy similar to the following:

$$n \cdot [Ca^{++}]_i + \text{Vesicles} \rightarrow \text{Release}$$

$$([Ca^{++}]_i)^n \cdot [\text{vesicles}] \cdot \text{rate constant} = \text{Rate of Release}$$

$$n \cdot \log([Ca^{++}]_i) + \text{Constant} = \log(\text{Rate of Release}).$$

The value of n has been evaluated by using changes of $[Ca^{++}]_o$ (43, 50) or I_{Ca} (17, 34) as approximations for changes in $[Ca^{++}]_i$. In the squid giant synapse all reported values for n range from one to two as determined by the slope of transmitter release to I_{Ca} (15, 17, 18, 22, 23). More recently a higher stoichiometry has been reported using pipette delivery for $[Ca^{++}]_o$ (51). A slope greater than 1 on the log-log plot was assumed to mean a stoichiometry greater than one for calcium ions in the release process (17, 33). However, as the membrane is depolarized from rest, and the macroscopic I_{Ca} increases, the microscopic flux per channel decreases. As a consequence, our modeling predicts an approximately inverse relationship between I_{Ca} and $[Ca^{++}]_i$ and that a stoichiometry of Ca^{++} to release of >1 should produce a slope of <1 on a plot of log (release) as a function of log (I_{Ca}). Furthermore, the results of the model indicate that if a stoichiometry >1 is assumed, a voltage modulation of transmitter release that is opposite to that actually observed is encountered.

While this linearity between $[Ca^{++}]_i$ and transmitter release may seem surprising a priori, given the widely accepted view that transmitter release is a cooperative phenomenon (17, 33, 43, 50), a linear relation is consistent with several experimental results in this preparation. Thus, if the stochiometry of $[Ca^{++}]_i$ to release were >1, then a shift of the resting free calcium level should shift the observed stoichiometry between calcium influx and release. For example, if the stoichiometry of $[Ca^{++}]_i$-to-release were four and the resting free calcium were increased, some of the binding sites for release would be occupied and the observed stoichiometry of a subsequent calcium influx-to-release should be decreased. In contrast, reducing the resting free calcium ion level should increase the stoichiometry up to the limit of four. When the resting potential of presynaptic terminal of the squid stellate ganglion is shifted in the depolarizing direction by an outward direct current (dc) injection, there is a continuous release of transmitter and a sustained presynaptic I_{Ca} (22, 52, 53), indicating a continuous increase of $[Ca^{++}]$ in the immediate submembranous compartment. However, there is no effect on the stoichiometry of the relationship between the I_{Ca} and transmitter release produced by a subsequent short duration depolarizing test pulse (52). This lack of change in the stoichiometry of release argues strongly in favor of a linear relation between $[Ca^{++}]_i$ and release.

The increase of $[Ca^{++}]_i$ also results in a substantial facilitative increase in the amount of transmitter release by the test pulse (51, 52), but the stoichiometry of the calcium

influx to release remains linear. The gain of the relation is increased as if the shift of the residual free calcium has a multiplicative effect on release by a subsequent calcium influx. This result is consistent with a model for which facilitation is the result of an increase in the number of vesicles available for release (41, 52, 53). The effect increases in magnitude over hundreds of milliseconds and lasts for hundreds of milliseconds after the resting $[Ca^{++}]_i$ is shifted (53). Thus we may conclude that the entry of calcium ions has at least two effects on transmitter release: a short term effect directly on release which is linearly dependent on calcium and a slower, longer lasting effect on the number of vesicles available for release at a given time (52).

Most previous studies on the stoichiometry of $[Ca^{++}]$ to release have been based on the effects of varying $[Ca^{++}]_o$. However, an increase of $[Ca^{++}]_o$ has at least two effects. It both increases the calcium influx during a test pulse, thereby increasing transmitter release, and increases the small resting calcium influx, thereby facilitating the calcium release by the test pulse. This would result in power dependence >1 for release based on varying $[Ca^{++}]_o$, even though the stochiometry of cytosolic calcium ions to release may be linear.

We thus suggest that two important factors should be considered when evaluating experimental results to determine the stoichiometry of the relation between cytosolic calcium and release. First the nonlinearity of the relationship between macroscopic I_{Ca} and the magnitude of $[Ca^{++}]_i$. Second, if the $[Ca^{++}]_i$ is changed other than with short duration influxes of I_{Ca} then the results may be complicated by secondary and tertiary effects of calcium on the release apparatus.

The Issue of Calcium Concentration vs. Release

Historically it has been assumed that vesicular release may be implemented by calcium concentrations not too far from the resting cytosolic $[Ca^{++}]_i$ levels. There is good evidence from the direct determination for the $[Ca^{++}]_i$ required for release at either adrenal medullary cells or sea urchin eggs (55–56), that $[Ca^{++}]_i$ in the order of micromoles is already capable of triggering release. Our modeling results suggest that at the presynaptic active zone, concentrations one to two orders of magnitude higher are attained during release. While this result could be viewed as paradoxical, by allowing $[Ca^{++}]_i$ to increase quite rapidly and over a very wide range, at a specific site, the release mechanism may be triggered into action much faster than it would otherwise. This would be in agreement with the work on adrenal medullary cells or sea urchin eggs (55–56) where the speed of release is directly related to $[Ca^{++}]_i$. The above assumption is also in keeping with a close to first-order relationship between $[Ca^{++}]_i$ and transmitter release observed at physiological $[Ca^{++}]_o$ and suggests that the secretory process may take place within a range of $[Ca^{++}]_i$ from tens to hundreds of micromoles at the active zone.

Possible Explanations for the Nonlinear Relationship between I_{Ca} and Transmitter Release

The morphological organization of the active zone suggests two explanations for the increased rate of transmitter release with increasing calcium influx. First, because the consequences of vesicular replacement time are more obvious at smaller than at larger depolarizations (Fig. 5), this difference results in a larger release of transmitter by a given I_{Ca} at larger depolarization. Thus, the positive voltage modulation in the relation between the presynaptic I_{Ca} and the rate of transmitter release (Fig. 5 *D*) and an apparent positive cooperativity between I_{Ca} and the rate of transmitter release (Fig. 5 *E*) can be viewed as due to the different distribution of open calcium channels at the two depolarizing levels in agreement with the nonlinear effect of voltage on depletion previously suggested in this preparation (41). Second, it is possible that release requires more than one channel to be simultaneously open in the immediate vicinity of a vesicle. This assumption produces a positive voltage modulation (Fig. 6 *A*) and apparent positive cooperativity between I_{Ca} and release.

Although they need not be mutually exclusive, the two explanations for the nonlinear relation between I_{Ca} and release suggested by the model can be experimentally distinguished by their predicted time courses. The depletion model predicts that the time dependence for the onset of the voltage modulation and the time course of depletion are related. If the I_{Ca} is short relative to the refractory period for vesicle replacement, then the depletion phenomena will not fully develop. The modulation will increase with pulse duration and stabilize with a time course close to that of the refractory period (i.e., >3 ms). By contrast the onset of the nearest neighbor effect will parallel the time course for the onset of I_{Ca} during a pulse (i.e., <2 ms).

We have assumed that a time lag for the transport of new vesicles to the subsynaptic membrane will generate this refractory period. This assumption fits well in the development of our modeling results relating to the distribution of the changes of submembrane calcium concentration. However, the model does not depend on this particular mechanism. The delays could be introduced by other events such as a time delay at a release site or at some other step in the release mechanism.

CONCLUSIONS

Transient changes of submembranous $[Ca^{++}]_i$ regulate many cellular phenomena. Different studies have examined the rate of secretion, synaptic depletion or facilitation as a function of either changes in $[Ca^{++}]_o$, changes of the transmembrane I_{Ca}, or average changes of $[Ca^{++}]_i$ (as

measured by dyes or ion-selective electrodes). These have produced complex relationships and complex models.

The present model of calcium influx through discrete channels predicts that (*a*) the resulting cytosolic increases of $[Ca^{++}]_i$ are highly localized spatially and temporally, and (*b*) there is a nonlinear relationship between the macroscopic I_{Ca} and magnitude of the submembrane $[Ca^{++}]_i$. As the membrane potential is depolarized, the macroscopic I_{Ca} increases as calcium channels open but the microscopic current through individual channels and the submembrane $[Ca^{++}]_i$ decrease due to a decrease in the electrochemical driving force for calcium.

Concerning transmitter release, the following are suggested by our modeling: (*a*) The time course and magnitude of transmitter release are linearly dependent on the highly localized changes in $[Ca^{++}]_i$. (*b*) Voltage effects on the distribution of calcium influx may underlie the experimentally observed properties of transmitter depletion. (*c*) The experimentally described nonlinearities between calcium entry and postsynaptic response can be accounted for either by the nonlinearities of depletion or by assuming that a vesicle must be exposed to calcium entry from more than one channel.

Thus, many of the apparent nonlinear properties of transmitter release may be the result of the manner in which the results have been examined. A model that accounts for the effects of membrane depolarization on the distribution of the calcium influx can predict these nonlinearities. Therefore, application of the predicted $[Ca^{++}]_i$ to synaptic physiology affords a clarification of our theories of calcium function. Assuming that I_{Ca} enters in a discrete manner, the compartmentalization of calcium entry is most probably a general principle for all calcium-dependent cellular functions. Together with the evidence that calcium channels may be aggregrated into patches (6), it suggests that the site of calcium entry is one of the significant parameters that determine its ultimate biological role. Future research on the role of calcium in cellular function should thus take into account present knowledge regarding the microscopic submembrane changes of $[Ca^{++}]_i$ rather than only extracellular $[Ca^{++}]_o$ changes, macroscopic I_{Ca}, or macroscopic $[Ca^{++}]_i$ changes.

The work was supported by United States Public Health Service grant NS-14014 from the National Institute of Neurological and Communicative Disorders and Stroke.

Received for publication 2 November 1985 and in final form 19 April 1985.

REFERENCES

1. Thomas, M. V. 1982. Techniques in Calcium Research. Academic Press Inc., London.
2. Nicola Siri, L., J. A. Sanchez, and E. Stefani. 1980. Effect of glycerol treatment on the calcium current of frog skeletal muscle. *J. Physiol. (Lond.).* 305:87–96.
3. Llinás, R., and R. Hess. 1976. Tetrodotoxin-resistant dendritic spikes in avian Purkinje cells. *Proc. Natl. Acad. Sci. USA.* 73:2520–2523.
4. Llinás R., and M. Sugimori. 1979. Calcium conductances in Purkinje cell dendrites: Their role in development integration. *Prog. Brain Res.* 51:323–334.
5. Katz, B., and R. Miledi. 1967. A study of synaptic transmission in the absence of nerve impulses. *J. Physiol. (Lond.).* 192:407–436.
6. Pumplin, D. W., T. S. Reese, and R. Llinás. 1981. Are the presynaptic membrane particles the calcium channels? *Proc. Natl. Acad. Sci. USA.* 78:7210–7213.
7. Brigant, J. L., and A. Mallart. 1982. Presynaptic currents in mouse motor endings. *J. Physiol. (Lond.).* 333:619–636.
8. Dunlap. K. 1976. Calcium channels in *Paramecium* confined to ciliary membrane. *Am. Zool.* 16:185.
9. Dunlap, K. 1976. Location of calcium channels in *Paramecium caudatum. J. Physiol. (Lond.).* 271:119–133.
10. Ogura, A., and K. Takahashi. 1976. Artificial deciliation causes loss of calcium dependent responses in *Paramecium. Nature (Lond.).* 264:170–172.
11. Strickhartz, G., R. Small, C. Nicholson, K. H. Pfenninger, and R. Llinás. 1980. Ionic mechanisms for impulse propagation in growing nonmyelinated axons: Saxitoxin binding and electrophysiology. *Soc. Neurosci. Abst.* 6:660.
12. MacVicar, B., and R. Llinás. 1982. Calcium spikes in regenerating giant axons of the lamprey spinal cord. *Soc. Neurosci. Abst.* 12:914.
13. Anglister, L., I. C. Farber, A. Shahar, and A. Grinvald. 1982. Localization of voltage-sensitive calcium channels along developing neurites: Their possible role in regulating neurite elongation. *Develop. Biol.* 94:351–361.
14. Freeman, J. A., B. G. Mayes, J. Snipes, and J. P. Wikswo. 1982. Real-time measurements of minute neuronal currents with a circularly vibrating microprobe. *Soc. Neurosci. Abst.* 12:302.
15. Llinás, R., I. Z. Steinberg, and K. Walton. 1976. Presynaptic calcium currents and their relation to synaptic transmission: Voltage clamp study in squid giant synapse and theoretical model for the calcium gate. *Proc. Natl. Acad. Sci. USA.* 73:2918–2922.
16. Llinás, R., I. Z. Steinberg, and K. Walton. 1981. Presynaptic calcium currents in squid giant synapse. *Biophys. J.* 33:289–322.
17. Charlton, M. P., S. J. Smith, and R. S. Zucker. 1982. Role of presynaptic calcium ions and channels in synaptic facilitation and depression at the squid giant synapse. *J. Physiol. (Lond.).* 323:173–193.
18. Augustine, G. J., and R. Eckert. 1984. Divalent cations differentially support transmitter release at the squid giant synapse. *J. Physiol. (Lond.).* 346:257–271.
19. Llinás, R., and M. Sugimori. 1978. Double voltage clamp study in squid giant synapse. *Biol. Bull. (Woods Hole).* 155:454.
20. Takeuchi, A., and N. Takeuchi. 1962. Electrical changes in pre- and postsynaptic axons of the giant synapse of *Loligo. J. Gen. Physiol.* 45:1181–1193.
21. Gage, P. W., and J. W. Moore. 1969. Synaptic currents at the squid giant synapse. *Science (Wash. DC).* 166:510–511.
22. Llinás, R., I. Z. Steinberg, and K. Walton. 1981. Relationship between presynaptic calcium current and postsynaptic potential in squid giant synapse. *Biophys J.* 33:323–352.
23. Llinás, R., M. Sugimori, and S. M. Simon. 1982. Transmission by presynaptic spike-like depolarization in the squid giant synapse. *Proc. Natl. Acad. Sci. USA.* 79:2415–2419.
24. Miledi, R., and I. Parker. 1981. Calcium transients recorded with arsenazo III in the presynaptic terminal of the squid giant synapse. *Proc. R. Soc. Lond. B. Biol. Sci.* 212:197–211.
25. Katz, B. 1969. The Release of Neural Transmitter Substances. Charles C. Thomas, Springfield, IL. 60 pp.
26. Simon, S. M., M. Sugimori, and R. Llinás. 1984. Modelling of submembranous calcium-concentration changes and their relation

to rate of presynaptic transmitter release in the squid giant synapse. *Biophys. J.* 45(2, Pt. 2):264*a*. (Abstr.)
27. Crank, J., and P. Nicolson. 1947. A practical method for numerical evaluation of solutions of partial differential equations of the heat conduction type. *Proc. Cambridge Phil. Soc.* 43:50–67.
28. Smith, G. D. 1978. Numerical Solution of Partial Differential Equations. 2nd edition. Clarendon Press, Oxford. 166 pp.
29. Lux, H. D. 1983. Observations on single calcium channels: An overview. *In* Single-Channel Recording. B. Sakmann and E. Neher, editors. Plenum Publishing Corp., New York. 437–449.
30. Baker, P. F., and W. W. Schlaepfer. 1978. Uptake and binding of calcium by axosplasm isolated from giant axons of *Loligo* and *Myxicola*. *J. Physiol. (Lond.)*. 276:103–125.
31. Connor, J. A., and G. Nikolakopoulou. 1982. *Lect. Math. Life Sci.* 15:1–19.
32. Llinás, R. R., and J. E. Heuser. 1977. Depolarization-release coupling systems in neurons. *Neurosci. Res. Program Bull.* 15:557–687.
33. Zucker, R. S., and N. Stockbridge. 1983. Presynaptic calcium diffusion and the time courses of transmitter release and synaptic facilitation at the squid giant synapse. *J. Neurosci.* 3:1263–1269.
34. Stockbridge, N., and J. W. Moore. 1984. Dynamics of intracellular calcium and its possible relationship to phasic transmitter release and facilitation at the frog neuromuscular junction. *J. Neurosci.* 4:803–811.
35. Parnas, H., and L. A. Segal. 1980. A theoretical study of calcium entry in nerve terminals, with application to neurotransmitter release. *J. Theor. Biol.* 91:125–169.
36. Safford, R. E., and J. B. Bassingthwaighte. 1977. Calcium diffusion in transient and steady states in muscle. *Biophys. J.* 20:113–136.
37. Gorman, A. L. F., and M. V. Thomas. 1980. Intracellular calcium accumulation during depolarization in a molluscan neurone. *J. Physiol. (Lond.)*. 308:259–285.
38. Fischmeister, R., and M. Horackova. 1983. Variation of Intracellular Ca^{2+} following Ca^{2+} current in heart. A theoretical study of ionic diffusion inside a cylindrical cell. *Biophys. J.* 41:341–348.
39. Chad, J., R. Eckert, and D. Ewald. 1984. Kinetics of calcium-dependent inactivation of calcium current in voltage-clamped neurones of *Aplysia californica*. *J. Physiol. (Lond.)*. 347:279–300.
40. Crank, J. 1975. *The Mathematics Of Diffusion.* 2nd edition. Clarendon Press, Oxford. 414 pp.
41. Kusano, K., and E. M. Landau. 1975. Depression and recovery of transmission at the squid giant synapse. *J. Physiol. (Lond.)*. 245:13–32.
42. Llinás, R. 1977. Calcium and transmitter release in squid synapse. *Soc. Neurosci. Symposia.* 2:139–160.
43. Katz, B., and R. Miledi. 1968. The role of calcium in neuromuscular facilitation. *J. Physiol. (Lond.)*. 19:481–492.
44. Rahamimoff, R. 1968. A dual effect of calcium ions on neuromuscular facilitation. *J. Physiol. (Lond.)*. 195:471–480.
45. Magleby, K. L., and J. E. Zengel. 1975. A quantitative description of tetanic and post-tetanic potentiation of transmitter release at the frog neuromuscular junction. *J. Physiol. (Lond.)*. 245:183–208.
46. Parnas, H., and L. A. Segal. 1980. A theoretical explanation for some effects of calcium on the facilitation of neurotransmitter release. *J. Theor. Biol.* 84:3–29.
47. Hodgkin, A. L., and R. D. Keynes. 1957. Movements of labelled calcium in squid giant axons. *J. Physiol. (Lond.)*. 138:253–281.
48. Baker, P. F., A. L. Hodgkin, and E. B. Ridgway. 1971. Depolarization and calcium entry in squid giant axons. *J. Physiol. (Lond.)*. 218:709–755.
49. Meves, H., and W. Vogel. 1973. Calcium inward currents in internally perfused giant axons. *J. Physiol. (Lond.)*. 235:225–265.
50. Dodge, F. A., and R. Rahamimoff. 1967. Cooperative action of calcium ions in transmitter release at the neuromuscular junction. *J. Physiol. (Lond.)*. 193:419–432.
51. Smith, S. J., G. J. Augustine, and M. P. Charlton. 1985. Transmission at voltage-clamped giant synapse of the squid. Evidence for cooperativity of presynaptic calcium action. *Proc. Natl. Acad. Sci. USA.* 82:622–625.
52. Simon, S. M., and R. R. Llinás. 1984. Residual free calcium hypotheses may not account for facilitation of transmitter release in the squid giant synapse. *Soc. Neurosci. Abst.* 10:194.
53. Simon, S. M., M. Sugimori, and R. Llinás. 1983. Resting potential affects transmitter release in the squid giant synapse. *Biophys. J.* 41(2, Pt. 2):136*a*. (Abstr.)
54. Means, A. R., and J. R. Dedman. 1980. Calmodulin—an intracellular calcium receptor. *Nature (Lond.)*. 284:73–77.
55. Knight, D. E., and P. F. Baker. 1982. Calcium-dependence of catecholamine release from bovine adrenal medullary cells after exposure to intense electric fields. *J. Membr. Biol.* 68:107–140.
56. Baker, P. F., D. E. Knight, and M. J. Whitaker. 1980. The relation between ionized calcium and cortical granule exotytosis in eggs of the sea urchin *Echinus esculentus*. *Proc. R. Soc. Lond. B. Biol. Sci.* 207:149–161.